Green Chemistry

Accepted Manuscript

ROYAL SOCIETY OF CHEMISTRY

www.rsc.org/greenchem

Manuscript for submitting to *Green Chemistry*

Understanding the Role of Water during Ionic Liquid Pretreatment of Lignocellulose: Co-solvent or Anti-solvent?

Jian Shi[1,2], Kanagasabai Balamurugan[3], Ramakrishnan Parthasarathi [1,2], Noppadon Sathitsuksanoh[1], Sonny Zhang[1], Vitalie Stavila[1,2], Venkatasen Subramanian[3], Blake A. Simmons[1,2], and Seema Singh[1,2,*]

[1]Deconstruction Division, Joint BioEnergy Institute, Emeryville, CA

[2]Biological and Materials Science Center, Sandia National Laboratories, Livermore, CA

[3]Chemical Laboratory, CSIR-Central Leather Research Institute, Adyar, Chennai 600 020, India

*Corresponding Author: E-mail: seesing@sandia.gov;

Fax: +1 510-486-4252; Tel: +1 925-294-4551

Abstract

Biomass pretreatment with certain ionic liquids (IL) can be highly effective at generating a substrate that can be easily saccharified into fermentable sugars with high yields. In order to improve overall process economics, using mixtures of these ILs with water is more favored over the use of anhydrous IL; however, the solvent property of IL-water mixtures and correlations between cellulose digestibility, cellulose solvation and lignin depolymerization during IL-water pretreatment of lignocellulosic biomass are not well understood. We investigated pretreatment of switchgrass with mixtures of 1-ethyl-3-methylimidazolium acetate, [C_2mim][OAc], and water at 160 $^{\circ}$C. Results indicate that the chemical composition and crystallinity of the pretreated biomass, and the corresponding lignin dissolution and depolymerization, were dependent on [C_2mim][OAc] concentration that correlated strongly with cellulose digestibility. In addition, the hydrogen bond basicity of the [C_2mim][OAc]-water mixtures was found to be a good indicator for cellulose dissolution, lignin depolymerization, and sugar yields. Molecular dynamics simulations provided molecular level explanations on cellulose I_β dissolution at different [C_2mim][OAc]-water loading. The knowledge gained from this study provides better understanding into the duality of water as a co-solvent/anti-solvent in dissolving cellulose and serves a design basis for the targeted design of IL-water mixtures that are effective at biomass pretreatment.

Keywords: pretreatment, aqueous ionic liquid, XRD, ^{13}C CP/MAS NMR, molecular dynamics

1. Introduction

Liberating fermentable sugars from lignocellulosic biomass economically opens avenues for commercial scale production of biofuels and chemicals. However, the recalcitrance of biomass to enzymatic degradation poses a barrier to economical biochemical conversion technologies, thus several physical and/or chemical pretreatment processes have been implemented to disrupt the recalcitrant lignocellulosic complex and improve enzymatic digestibility [1, 2]. As an emerging technology, pretreatment using certain ionic liquids (ILs), such as 1-ethyl-3-methylimidazolium acetate ([C_2mim][OAc]), shows superior performance compared to several other pretreatment technologies in terms of dramatically reducing biomass recalcitrance and enhancing enzymatic hydrolysis to fermentable sugars [3-5]. The main challenges facing IL pretreatment are the cost of ILs and system complexity associated with IL recycle, biomass solute separation and downstream processing [6, 7].

Relying on the recent development of a thermophilic and IL-tolerant biomass-deconstructing enzyme cocktail, called JTherm [8, 9], we have developed a one-pot wash-free pretreatment and saccharification process that enables high sugar yields being achieved in the presence of 10-20% [C_2mim][OAc] IL remaining after pretreatment [5]. More recent studies have shown that lower IL concentrations (10-50% w/v) in water may also be effective in pretreating biomass, potentially reducing the amount of washing required prior to enzymatic saccharification [10-12]. Furthermore, using IL-water mixtures as pretreatment agents could reduce viscosity, eliminate gel formation during pretreatment and reduce the energy inputs and costs associated with IL recycle, facilitating scale-up and downstream processing.

To date, there are relatively few papers on the interactions between cellulose and IL-water mixtures during cellulose regeneration after pretreatment [13, 14]. Water has been considered as the driving force for separating cellulose from IL upon the addition of water as an anti-solvent [13] and addition of up to 21 wt% water to [C_2mim]Cl-cellulose solution initiates cellulose precipitation [15]. It is also reported that the addition of water leads to the perturbation of cellulose---$[OAc]^-$ hydrogen-bonds (H-bonds) and the cellulose-cellulose interaction is enhanced at elevated temperatures [16]. Recently, Huo et al. examined the role of ILs, DMSO, water and mixed solvent systems on solvation or regeneration of I_β cellulose crystal [17]. Water, itself, as a pretreatment medium, can extract native hemicelluloses; at elevated temperature acetic acid is quickly liberated, further increasing hemicellulose yields, a well documented "auto-hydrolysis" phenomena reported in literature [2]. Hydrogen-bond basicity of the solvent system provides a direct indication of IL pretreatment efficacy, producing greater lignin/xylan removal, reduced cellulose crystallinity and improved enzymatic digestibility [18, 19].

Previous studies have demonstrated that comparable sugar yields can be achieved at reduced IL loading (<50%) in water at elevated temperatures. However, at higher temperature during IL-water pretreatment, the interplay of water as pretreatment medium (co-solvent) and as anti-solvent has not been comprehensively explored. In this study, we further define the role of water during ionic liquid-water pretreatment of lignocellulose as either a co-solvent or anti-solvent. We conducted pretreatment of microcrystalline cellulose (Avicel) and switchgrass with 0, 20, 50, 80, and 100 wt% 1-ethyl-3-methylimidazolium acetate, [C_2mim][OAc], with corresponding amounts of water, at 160 $^\circ$C for 3h. The chemical composition, crystallinity and cellulose accessibility of pretreated biomass were monitored at different IL loadings and correlated to cellulose digestibility. Furthermore, Kamlet-Taft (K-T) parameters were used to predict cellulose

dissolution and lignin depolymerization and correlated to sugar yields. Molecular dynamics simulations of an atomistic model of cellulose I_β dissolution at different [C_2mim][OAc]:water loading at set temperatures were used to simulate the experimental conditions studied. This combination of experimental and computational study provides new insight into the role of water during [C_2mim][OAc] pretreatment and provides base for the development of a more cost-effective route for the production of fermentable sugars from lignocellulose.

2. Results and discussion

2.1 Compositional changes

Chemical composition, solid recovery, and component removal of switchgrass before and after pretreatment with ionic liquid-water mixtures are summarized in Table 1. Pretreatment with 100% IL removed the greatest amount of biomass fractions (resulted in the lowest solid recovery of 49.3%), while reducing [C_2mim][OAc] loading led to higher solid recovery, with 20:80 [C_2mim][OAc]:H_2O mixture and water-only pretreatments recovering >59% of the biomass. Solids pretreated with 100% [C_2mim][OAc] had the highest glucan content while the water-only has the least. In general, all pretreated solids retained ~90% of the initial glucan content. In contrast, large amount of xylan was removed during pretreatment; with solids pretreated with 100% [C_2mim][OAc] contains the lowest xylan contents in accordance to the greatest xylan removal of 78.8%. Water-only pretreatment also removed large amount of xylan, due to the "auto-hydrolysis" effects caused by the release of acetic acid during pretreatment, a phenomenon well documented in literature [2]. Interestingly, pretreatment with 20-50% [C_2mim][OAc] was less effective on xylan removal compared with pretreatments at either higher [C_2mim][OAc] concentration or water only. We speculate that in this range the [C_2mim][OAc] provided a

103 buffering capacity to the pH decrease associated with the release of acetic acid during
104 pretreatment [20], and thus reduced the extent of xylan solubilization from "auto-hydrolysis"
105 effects, as indicated by the nearly neutral pH of the biomass liquor generated (Table 1).

106 ILs based on imidazolium cations, such as 1-allyl-3-methylimidazolium chloride ([C_1mim] Cl),
107 1-n-butyl-3-methylimidazolium chloride ([C_4mim]Cl), and [C_2mim][OAc], possess an excellent
108 capacity for dissolving cellulose partially owing to the high hydrogen-bond basicity of these ILs
109 [7]. Furthermore, associated with cellulose dissolution, many studies have shown simultaneous
110 removal of xylan and lignin owing to the interruption of hydrogen bonding within cellulose,
111 hemicelluloses and lignin [4, 7]. It has been demonstrated that [C_2mim][OAc] can effectively
112 breakdown of G- and S-lignin during IL pretreatment dependent on both pretreatment conditions
113 and the type of biomass feedstocks [21, 22]. Results show less lignin removal during pretreatment
114 with 20% [C_2mim][OAc] mixture compared with that of 100% [C_2mim][OAc]. Water-only
115 pretreatment removed 11.5% (the least) of lignin. Pretreatment with 50-80% [C_2mim][OAc] can
116 remove more than 50% of the lignin from raw switchgrass, only slightly less than that of 100%
117 [C_2mim][OAc].

118 *2.2 Changes of cellulose crystallinity*

119 The proportions of crystalline/amorphous cellulose and the disordered components (i.e.
120 amorphous cellulose, hemicelluloses and lignin) found in pretreated switchgrass samples were
121 determined by pXRD and expressed as crystallinity index (CrI). Except for switchgrass
122 pretreated with 100% [C_2mim][OAc] (showing transition to cellulose II), all the samples
123 pretreated with IL-water mixtures or water-only are semi-amorphous and retain primarily
124 cellulose I structure with different degrees of CrI (Figure 1a). Switchgrass pretreated with 100%

[C_2mim][OAc] has the lowest CrI value (16%) compared with the CrI of 0.36 of untreated switchgrass, due to the partial swelling of the cellulose matrix by [C_2mim][OAc]. Switchgrass pretreated with water-only has increased CrI value of 0.39 compared to raw switchgrass, an effect attributed to the removal of amorphous lignin and hemicelluloses. While for solids after [C_2mim][OAc]-water pretreatment, the CrI decreases as the ratio of [C_2mim][OAc] increases in solution. The mechanism behind the CrI changes during [C_2mim][OAc]-water pretreatment process may be determined by two competing factors: 1) swelling and dissolution of the cellulose portion (a decrease of CrI); 2) removal of the amorphous lignin and hemicelluloses (an increase of CrI). The increase in CrI values after water-only pretreatment indicates that lignin and hemicellulose removal is the dominating mechanism, an observation consistent with the compositional analysis (Table 1). Nevertheless, decrease in CrI after pretreatment with 50-80% [C_2mim][OAc] mixture indicates that swelling and dissolution of the cellulose (reduction in CrI) outplays the removal of amorphous components (increase in CrI). The CrI of solids resulted from pretreatment with 20% [C_2mim][OAc] remains unchanged, likely representing a balance in the two driving factors: both dissolution of the cellulose and removal of amorphous xylan and lignin (Table 1).

To further understand cellulose structural changes during pretreatment with [C_2mim][OAc]-water mixtures, Avicel was pretreated at the same conditions and the XRD spectra were plotted in Figure 1b. After pretreating Avicel in 100% [C_2mim][OAc], cellulose I has been completely transformed to cellulose II as displayed in XRD patterns of the characteristic diffraction peaks at ~ 12.1°, 20.0°, and 21.7° [23, 24]. In contrast, the crystalline structure of Avicel pretreated with water-only remained the same as untreated Avicel (i.e. cellulose I and amorphous). However, the crystalline structures of Avicel pretreated with IL-water mixtures showed partial features of both

148 cellulose I/amorphous and cellulose II. It is also seen that a clear trend of decrease in CrI follow
149 the ratio of IL in the water solution. These results indicate that although [C_2mim][OAc] is
150 capable of dissolving or swelling cellulose, the presence of water, as anti-solvent, conversely,
151 decrease the effectiveness of cellulose dissolution and retards the transformation of cellulose I to
152 amorphous/cellulose II.

153 *2.3 Solvent properties of [C_2mim][OAc]-water mixtures*

154 Certain solvent properties, such as solvatochromic properties, describe solute-substrate hydrogen
155 bonding interactions. The Kamlet-Taft system bins these properties into three separate terms:
156 polarizability (π*), hydrogen bond donator capacity (α) and hydrogen bond acceptor capacity (β)
157 [25]. Although the Kamlet-Taft procedure was initially designed for measuring solvent properties
158 of a single solvent, it has been applied to describing the average or bulk solvent properties of
159 binary and ternary solvent mixtures [11, 26]. The solvent properties of the [C_2mim][OAc]-water
160 mixtures studied are summarized in Table 2. We found that π* decreased as water content
161 increased. Similar behavior was observed for β; these values have been considered to be a good
162 predictor of IL pretreatment efficacy with higher β (>1.0) values correlated to: 1) greater
163 lignin/xylan removal; 2) reduced cellulose crystallinity and 3) improved enzymatic digestibility.
164 Doherty et al. [27] have proposed that ILs with higher β values form strong attractions between
165 anions and the hydroxyl protons of cellulose, leading to disruption of the crystal lattice. In
166 addition, Sun and co-workers (2014) established links between computationally predicted
167 interaction energies and the experimentally determined Kamlet-Taft parameters and showed a
168 positive correlation between glucose yield and β values [19]. Results from this study suggest that
169 the same rules may apply to pretreatment with IL-water mixtures, with positive linear
170 correlations observed between β values and lignin removal and initial glucose yield (Figure 4).

As reported previously, the β value is primarily determined by the anion [28-30] and ILs with higher β values [31], and more recently ILs with larger differences between β and α, net basicity (β-α) [32, 33], tend to dissolve cellulose more efficiently. Our results suggest that although the β values decreased for IL-water mixtures as a function of water content, it can be used to predict the pretreatment efficiency and define an effective range of concentrations to conduct pretreatment

2.4 Lignin dissolution and depolymerization

The differences seen in lignin removal and CrI patterns in the previous sections merited further investigation into the impacts of IL-water mixtures on lignin dissolution and depolymerization. Lignin dissolution caused by the cleavage of specific inter-unit lignin linkages and lignin carbohydrate cross-links has been widely investigated on water-only pretreatment [34-36]. The mechanism of lignin depolymerization during [C_2mim][OAc] pretreatment was recently examined [22, 37, 38] and preferential lignin dissolution was often observed due to the chemical nature of lignin according to building blocks and the inter-unit linkages [38]. In order to monitor the lignin molecular weight distribution as a function of pretreatment using different [C_2mim][OAc]-water content, size exclusion chromatography (SEC) were performed on lignin solublized in aqueous [C_2mim][OAc] and remained in pretreated solids (Figure S1). Excluded ($A_{Excluded}$) and retained ($A_{Retained}$) regions are defined using the retention time of 13.4 min (u = ~46k by polystyrene calibration). Decreases in the ratios of the relative area ($A_{Excluded/Retained}$ ($A_{E/R}$)) of the mass peak of larger molecular mass lignin products (t < 13.4 min) to smaller molecular mass lignin products (t > 13.4 min) for lignin fraction compared to that of enzymatic mild acidolysis lignin (EMAL), are a broad gauge for depolymerization. The $A_{E/R}$ were reported in Table 3 as an indicator of the relative molecule weight distribution of solublized lignin in aqueous [C_2mim][OAc] or lignin that remained in the solid stream. EMAL of untreated

switchgrass samples showed a strong signal in the excluded region (t < 13.4 min) with an $A_{E/R}$ of 2.43, suggesting that EMAL of untreated switchgrass consisted mainly of large molecular weight materials. As for the lignins solublized in IL-water during pretreatment, a distinct signal in the retained region (t > 13.4 min) was observed with reduced $A_{E/R}$ in a range of 0.46 to 0.92 for different [C_2mim][OAc]-water mixtures compared to that of EMAL. The lower $A_{E/R}$ in solublized lignin indicates that lignin was solublized and depolymerized in the liquid stream during pretreatment [5, 39]. Interestingly, the $A_{E/R}$ for the lignin solublized in 100% [C_2mim][OAc] or water-only was lower than that solublized in 20-80% [C_2mim][OAc], indicating possible different lignin dissolution or depolymerization mechanisms.

The lignin residues in all pretreated solids showed higher $A_{E/R}$ (greater than 1) compared with the soluble lignin (less than 1). Furthermore, compared to EMAL of untreated switchgrass, residual lignin in pretreated solids exhibited lower $A_{E/R}$, indicating that the pretreated switchgrass contained smaller molecular weight material than the EMAL, supporting small molecular weight lignin materials observed in the liquid streams. It is possible that either branches or end-units have been removed from the recalcitrant lignin "backbone", reducing its molecular mass but not allowing it to fully solubilize, a phenomenon reported previously [39]. Moreover, $A_{E/R}$ of residual solids after 100% IL pretreatment was much smaller than that of residual solids pretreated by [C_2mim][OAc]-water mixtures, suggesting that adding water negatively influence the effectiveness of delignification and lignin depolymerization [19].

2.5 Cellulose accessibility and substrate characteristics

We used solid-state ^{13}C CP/MAS NMR in conjugation with FTIR spectra to evaluate the cellulose accessibility and substrate characteristics of [C_2mim][OAc]-water pretreated

switchgrass. The NMR spectrum reveals ^{13}C chemical shifts of cellulose carbons (Figure 2a), including C1 (105 ppm), C4 (79–92 ppm), C2/C3/C5 (70–80 ppm), and C6 (60–69 ppm) with the C4 and C6 resonance region commonly used for determining cellulose crystallinity [40-42]. The NMR spectrum of raw switchgrass showed strong signals at 89 and 65 ppm and broad signals at 83 and 63 ppm, indicating that raw switchgrass contains both crystalline and amorphous fractions, which is in agreement with that previously reported [43]. It is evident that the crystalline peaks decreased and the amorphous peaks increased in C4 and C6 regions for switchgrass samples treated by 100% [C_2mim][OAc], indicating that highly ordered hydrogen-bonding networks in switchgrass was disrupted by [C_2mim][OAc]. We also observed a gradual transition of crystalline and amorphous peaks of switchgrass pretreated with 0-100% [C_2mim][OAc], suggesting the gradual decreases of solvation power of [C_2mim][OAc]-water mixtures from high to low [C_2mim][OAc] concentrations. Comparison of FTIR spectra of [C_2mim][OAc]-water pretreated switchgrass shows differences in band intensities at 900 cm^{-1} (C-H deformation in cellulose), 1056 cm^{-1} (C-O stretching in cellulose and hemicelluloses), 1098 cm^{-1} (C-O vibration of crystalline cellulose), 1329 cm^{-1} (syringyl and guaiacyl condensed lignin), and 1510 cm^{-1} (Aromatic skeletal of lignin) cm^{-1} [4]. Figure 2b shows that the band intensities at 1056 and 1098 cm^{-1} decrease from raw switchgrass to 100% [C_2mim][OAc] pretreated switchgrass, implying that highly ordered hydrogen bonds in raw switchgrass were disrupted through cellulose dissolution and regeneration [43]. The 50-80% [C_2mim][OAc]-water pretreated sample showed more significant decreases in the band intensities at 1098, and 1056 cm^{-1} than raw SG, suggesting that highly ordered hydrogen bonds in crystalline cellulose of switchgrass were disrupted after the pretreatment.

2.6 Enzymatic digestibility

As expected, pretreatment with 100% IL led to very high cellulose digestibility when pretreated solids were subjected to enzymatic hydrolysis, at both low and high enzyme loadings (Figure 3). It is also noticed that the glucose yield curve enters plateau after 24h, a result matching previous reports on the nearly complete saccharification within 24 h [44]. The fast hydrolysis kinetics is due to the regeneration of easily digestible type II/amorphous cellulose when cellulose is treated with ionic liquid [4,24]. Interestingly, 85-90% glucose yields were achieved for pretreatment with 50-80% [C_2mim][OAc] at 20mg enzyme/g biomass. However, much lower glucose yields were seen for pretreatment with water-only or 20% [C_2mim][OAc]. Notably, fast sugar releases in the first 24h were also observed for solid pretreated with 50-80% [C_2mim][OAc] as compared with that of water-only pretreatment, indicating that these solids were readily saccharified. Results from study were in general agreement with previous reports using [C_2mim][OAc] and water as pretreatment media [10, 45]. However, higher than 85% glucose yield, within 24 hr, can only be achieved using 60-90% [C_4mim][$MeSO_4$] or [C_4mim][HSO_4] in water [11], indicating that the pretreatment efficiency is also dependent on the selection of ILs as well as the presence of water.

Associated with the compositional changes, it is inferred that the initial glucose yields (average % per hour glucose release in the first two hours) were positively correlated to lignin removal (Figure 4a). However, it seems that only at >50% lignin removal the initial glucose yields can be significantly increased, an observation that matches the high overall glucose yield and fast saccharification kinetics seen for pretreatment with 100% [C_2mim][OAc] or 50-80% [C_2mim][OAc] mixtures. Furthermore, there is a positive linear correlation between the initial glucose yields and β values, indicating that β values could be used to predict the pretreatment efficiency for [C_2mim][OAc]-water mixture (Figure 4b). No strong correlations were seen

between xylan removal/CrI and the initial glucose yields (Figure 4c&d), probably due to the very different mechanisms behind water-only pretreatment and pretreatment with 100% [C_2mim][OAc] or [C_2mim][OAc]-water mixtures. Although cellulose with a high amorphous content are usually more easily digested by enzymes, it is clear that CrI is not a reliable sole indicator of digestibility, especially for lignocellulosic biomass, based on studies published in the literature [42, 46]. Cellulose digestibility can be affected by crystallinity, but is also affected by several other parameters, such as lignin/hemicellulose contents and distribution, porosity, and particle size [2, 46].

2.7 Molecular dynamics simulation of cellulose dissolution in IL-Water mixture

Experimental and theoretical studies have been carried out to understand the interactions between cellulose and ILs [13, 47]. Cellulose chains form stronger interaction with the IL than with water. For instance, acetate anion forms strong hydrogen bonding interactions with the hydroxyl groups of cellulose and some of the cations were found to be in close contact with the cellulose through hydrophobic interactions [13]. In this work, classical MD simulation has been performed to gain an atomistic level understanding on the dissolution of cellulose model matrices composed of cellulose I_β in different [C_2mim][OAc] and water concentrations (Figure S2). The results of inter-chain and total H-bonds in the cellulose matrix during the course of simulation (Figure 5) show that the reduction in the number of H-bond is directly proportional to the concentration of [C_2mim][OAc] which is in accordance with the earlier reports [13]. It is interesting to note that the trend in the decrease of total H-bonds is similar to the inter-chain H-bonds. However, the close scrutiny of the plot of inter-chain H-bonds with time shows that there are no appreciable changes in the number of H-bonds observed in the case of simulation in 100%, 80%, and 50% [C_2mim][OAc]. The above results reveal that the dissolution of cellulose bundle into individual

cellulose chains in both 50% and 80% [C_2mim][OAc] in water is comparable to that of 100% [C_2mim][OAc]. Our results are in agreement with previous simulation on cellulose-IL dissolution, in which ILs influencing intermolecular and intramolecular interactions of cellulose [13] and also, complementary to the experimental trend reported here for different concentration of [C_2mim][OAc]-water mixture. It is well known that degree of polymerization (DP) influences the solvation. In the case of cellulose with DP < 6 are quite soluble in water and water solubility of cellulose decreases as the chain-length increases.[43] These results indicate that the dissolution of cellulose with DP= 6 occurs in accordance with concomitant solvation properties. However, the results may quantitatively vary with the higher DP.

Another important focus of our study is elucidating the role of water in cellulose dissolution of [C_2mim][OAc]. We carried out an additional analysis (Figure 6) of dissecting water interactions with anions, cations, and cellulose from different [C_2mim][OAc]-water mixtures. The water interaction with ions is typically one of the rate-limiting steps preceding regeneration of cellulose [32, 48]. This additional analysis has ramifications on the role of water interaction and its relationship to overall solvation efficiency in various [C_2mim][OAc]-water concentrations. We found that interaction energies of water with cellulose chains were increased gradually with the increase in the concentration of water, but interestingly, it enhanced interactions with [OAc] and [C_2mim] ions on 50% of water concentration. Results indicate that as IL-water mixtures less than 50% of water with [C_2mim][OAc] support dissolution of the cellulose model system simulated in this work, whereas water concentrations higher than 50% enhances interactions of water molecules with ions but weakens cellulose-[C_2mim][OAc] interactions. As illustrated in Fig. 6 on hydrogen bonding interactions with anion/cellulose, at lower concentration, water acts as (co-)solvent which help to facilitate the disintegration of strong ionic anion-cation association of

[C_2mim][OAc]. Moreover, taking into the consideration that water molecules strongly solvate the ions above 50% concentration, it conceivable that above that concentration breaking cellulose-[C_2mim][OAc] interactions for the most part saturating hydrogen bonding interactions of anions. Our simulation predicts that a reduction in the effective IL dissolution of cellulose coupled with an increase in the water concentration by increasing water molecule interactions with the anions and cations as well as cellulose (a schematic of the proposed IL-Water dissolution mechanism of cellulose Fig. S2). The present results thus suggest a synergistic solution on the limit of minimum/maximum [C_2mim][OAc]:water loading to improve the cellulose dissolving capability of ILs.

3. Conclusions

Our results showed that pretreatment with 50-80% [C_2mim][OAc] aqueous mixtures at 160 °C can match the performance of 100% [C_2mim][OAc] in terms of glucose yield. The ratio of [C_2mim][OAc] in water plays a critical role in cellulose solubilization, lignin and xylan removal, crystallinity, and cellulose accessibility, and in combination greatly affect the enzymatic digestibility. The hydrogen bond basicity (β value) representing the ability of disrupting the inter- and intra-molecular hydrogen bonding in cellulose, hemicellulose and lignin, correlates well with cellulose crystallinity, lignin removal and serves as a good indicator of pretreatment efficacy for [C_2mim][OAc]-water mixtures. Molecular dynamics simulations provided molecular level explanations on cellulose I_β dissolution at different [C_2mim][OAc]-water loadings at set temperatures which shows that IL-water mixtures can be efficiently used for the solubilization of cellulose microfibrils into individual chains. Our findings provide new insights into the interplay of water as a co- and anti-solvent, respectively, below and above 50% [C_2mim][OAc] concentration in the chosen model systems for the dissolution of cellulose. On considering the

importance of dissolution of cellulose bundle into individual chains for the efficient enzymatic hydrolysis of polysaccharides and taking into account of the cost of using IL, it is feasible to employ [C_2mim][OAc] in the range of 50-80% in water to achieve an efficient dissolution of cellulose in an economically viable process.

4. Experimental

4.1 Materials

Switchgrass (*Panicum virgatum*) was provided by Dr. Daniel Putnam, University of California at Davis. Switchgrass was ground by a Wiley Mill through a 2 mm screen and separated by a vibratory sieve system (Endecotts, Ponte Vedra, FL). The switchgrass fractions falling between 20 and 80 mesh were collected for use in this study. The moisture content of switchgrass was measured as 6.7%. Avicel PH101 (Lot No. 1344705, Sigma-Aldrich, St. Louis, MO), is a microcrystalline cellulose (MCC) containing more than 97% cellulose and less than 0.16% water soluble materials. 1-ethyl-3-methylimidazolium acetate, abbreviated hereafter as [C_2mim][OAc], was purchased from BASF (Basionics™ BC-01, BASF, Florham Park, NJ) and used as the IL for all pretreatments. The water content of [C_2mim][OAc] was measured as 0.7% using a titrator (870 KF Titrino plus, Metrohm USA Inc., Riverview, FL) and was counted to the final water concentration in [C_2mim][OAc]-water mixtures. Commercial enzyme products, cellulase (Cellic® CTec2, Batch#VCN10007) and hemicellulase (Cellic® HTec2, Batch#VHN00002) were gifts from Novozymes, North America (Franklinton, NC).

4.2 Pretreatment with IL:water mixtures

IL-water mixtures were prepared by mixing [C_2mim][OAc] with DI water at different ratios to give five levels (0, 20, 50, 80, 100 wt%, equivalent to 0, 0.024, 0.096, 0.297, and 1 mole fraction,

respectively) of IL in water. Two grams of switchgrass (dry basis) were mixed with 18 grams of [C_2mim][OAc]-water solution to give a 10 wt% biomass loading in tubular reactors made of 1 inch diameter × 4 inch length stainless steel (SS316) tubes. The tubes were then sealed with stainless steel caps. All pretreatments were run in triplicate in tubular reactors that were heated to reaction temperature using fluidized sand bath with temperature set circa 2 °C higher than the pretreatment temperature to hold the reaction at the target temperature as measured by a thermocouple. The heat up time was ~8-10 min and is not included in the stated reaction times. After pretreatment, the reactors were quenched by quickly transferring them to a room temperature water bath until the temperature dropped to 30°C (the cooling time was around 1-2 min and was not included in the stated reaction time).

To separate solids from liquid after pretreatment, the pretreated biomass was transferred to a 50 ml centrifuge tube and 20 ml hot water was added to the samples as anti-solvent for cellulose regeneration and for recovering any solublized biomass. The mixture of [C_2mim][OAc], water, and pretreated biomass was centrifuged to separate the solids and liquid phases. The liquid phase, namely pretreatment liquid, was collected and store at 4°C for sugar analysis. The solid fraction was washed four times with 45 ml of hot water to remove any excess [C_2mim][OAc]. An aliquot of recovered solid was lyophilized in a FreeZone Freeze Dry System (Labconco, Kansas City, MO) and used for composition and X-ray diffraction (XRD) analysis.

4.3 X-ray powder diffraction measurements

XRD data were collected with a PANalytical Empyrean X-ray diffractometer equipped with a PIXcel^{3D} detector and operated at 45 kV and 40 kA using Cu *Kα* radiation (λ= 1.5418 Å). The patterns were collected in the 2θ range of 5 to 55°, the step size was 0.026°, with an exposure

time of 600 seconds. A reflection-transmission spinner was used as a sample holder and the spinning rate was set at 8 rpm throughout the experiment. The crystallinity index (CrI) was determined from the crystalline and amorphous peak areas by a curve fitting procedure of the measured diffraction patterns using the software package HighScore Plus®. Since the XRD peak height method is unsuitable for determining the CrI values of cellulose II or cellulose I/II mixtures, we used the crystalline area method previously described eslewhere, using crystalline cellulose I (Avicel), cellulose II (prepared previously in our laboratory [24]) and amorphous (Lignin) as representative samples [42]. The CrI values reported in this study reflect the ratio of the areas of the crystalline fractions (with the amorphous component subtracted) to the total area of the measured XRD patterns.

4.4 Solid-state ^{13}C CP/MAS NMR and FTIR

The cross-polarization magic-angle spinning (CP/MAS) ^{13}C-NMR spectra of all samples were obtained on a Bruker II Avance-300 spectrometer operating at the resonance frequencies of 300.12MHz for 1H, and 75.47MHz for 13C, using a Bruker 4.0mm MAS NMR probe spinning at 6 kHz. Cross-polarization for 1ms mixing time was achieved at 50 kHz rf-field at the 1H channel and linearly ramping the 13C rf-field over a 25% range centered at 38 kHz. Total accumulation time was 8 min (2048 transient signals) by using 63 kHz of two-pulse phase modulated proton decoupling technique [49]. All spectra were collected at room temperature with polyethylene as an internal standard. According to the NMR amorphous subtraction method, amorphous contribution was separated from the original spectrum prior to deconvolution of signals in the C4 resonance region, where xylan was an amorphous standard [41].

4.5 Enzymatic hydrolysis

Enzymatic saccharification of pretreated and untreated biomass samples were run in duplicates by following NREL LAP 9 "Enzymatic Saccharification of Lignocellulosic Biomass" at NREL standard conditions (50 °C, 0.05 M citrate buffer, pH 4.8) [50]. Citrate buffer (final molarity 50 mM), sodium azide (antimicrobial, final concentration of 0.01 g/L), enzymes, and DI water were mixed with pretreated solids to achieve a final solids loading of around 5% (equivalent to 2.5 % (w/w) glucan concentration). CTec2 and HTec2, were used at enzyme loadings of 5 and 20mg CTec2 protein/g pretreated biomass supplemented with HTec2 at loadings of 0.07 and 0.26 mg enzyme protein/g glucan, respectively. The supernatant collected during 72 h of hydrolysis was analyzed with HPLC for the monosaccharide as described in the analytical method section below. Enzymatic digestibility was defined as the glucose yield based on the maximum potential glucose from glucan in biomass.

4.6 Analytical methods

The saccharification hydrolyzate was separated by centrifugation at 14,000×g for 10 min followed by syringe filtration. The amount of cellobiose, glucose, xylose, and arabinose released in the hydrolyzate was measured by Agilent 1100 series HPLC equipped with a Biorad Aminex HPX-87H ion exchange column and refractive index detector, using 4 mM H_2SO_4 as mobile phase at a flow rate of 0.6 ml min^{-1} and a column temperature of 60°C. Furthermore, for oligomers determination, an aliquant of pretreatment hydrolysate was mixed with an equal volume aliquant of 72% H_2SO_4, incubated at 30°C for 1h, diluted to 4% sulfuric acid concentration with DI water and autoclaved at 121°C for 1 hour (post-hydrolysis) according to NREL LAP "Determination of Sugars, Byproducts, and Degradation Products in Liquid Fraction

Process Samples" [51]. Differences between the amount of sugars following post-hydrolysis and the monomer content before post-hydrolysis were defined as the oligomeric sugar content.

4.7 Characterization of lignin in liquid and residual solids

To understand changes of lignin molecular weight distribution during the consolidated IL pretreatment and saccharification, size exclusion chromatography (SEC) were performed on the lignin in both liquid stream and residual solids after consolidated IL pretreatment and saccharification for 72 h. An Agilent 1200 series binary LC system (G1312B) equipped with DA (G1315D) detector was used. Separation was achieved with a Mixed-D column (5 μm particle size, 300 mm x 7.5 mm i.d., linear molecular weight range of 200 to 400,000 u, Polymer Laboratories, Amherst, MA) at 80°C using a mobile phase of NMP at a flow rate of 0.5 ml per min. Elution profile of materials eluting from the column was monitored by UV absorbance at 290 nm (UV-A_{290}). Intensities were area normalized and molecular weight were determined after calibration of the system with polystyrene standards [39]. Enzymatic mild acidolysis lignin (EMAL) process was used to extract lignin from switchgrass and used as a control [52].

4.8 Kamlet-Taft (K-T) parameters measurement

Parameters derived from the Kamlet–Taft procedure, namely K-T parameters, provides a quantitative measurement of solvent polarizability (π*), hydrogen bond donator capacity (α) and hydrogen bond acceptor capacity (β). K-T parameters were determined spectrophotometrically using a series of dyes according to previous reports [18, 27]. The three dyes: 4NA, DENA, and RD solutions were prepared in ethanol to a concentration of 1 mg/mL. 2 μL of 4NA, 2 μL of DENA and 20 μL of RD were pipetted into three separate vials and the ethanol was evaporated under a stream of dry nitrogen. Dye concentrations of 12 mM, 8 mM, and 28 mM respectively, were

obtained by adding 1.25mL of the appropriate ILs to each vial and mixing on a shaker at 300 RPM for 30 min. The absorbance spectra at 30, 60, 90, and 110 ºC of each IL/dye solution was measured between 350 and 700 nm using a spectrophotometer equipped with temperature controller (TMSPC-8, Shimadzu Corporation). K-T parameters for higher temperatures were estimated by using a linear regression of the parameter values between 30 and 110 ºC [22].

4.9 Computational Methods

Molecular dynamics simulation of the cellulose I_β with 9 chains was taken as a model system in which each chain has a degree of polymerization of 6 (6 glucose units). The cellulose was immersed in a box of size 34 X 48 X 52 Å and solvated with [C_2mim][OAc]/water solvent systems of various concentration (Water, 20%IL, 50%IL, 80%IL and 100%IL). MD simulations were carried out using Gromacs 4.6 suite of package [53, 54]. For the simulation, GLYCAM forcefield was used for the cellulose [55]. The GAFF parameters [56] with charges from Liu et al [13] were used for IL and the water molecules were treated using TIP3P parameters [57]. A 2 fs time step was used to integrate the equation of motion. Electrostatic interaction was calculated using Particle Mesh Ewald sums [58] with a nonbonded cut-off of 10 Å. Bonds between hydrogen and heavy atoms were constrained at their equilibrium length using the LINCS algorithm [59]. Equilibration was performed for of 250 ps in NVT ensemble and the temperature was increased from 300 to 433K. Further, 500 ps of equilibration was carried out in NPT ensemble. Subsequently, 100 ns of production run was carried out in NPT ensemble for all the systems. The pressure was retained at 1atm and temperature was retained at 433K using Parrinello-Rahman barostat and V-rescale thermostat, respectively [60]. The trajectories were saved every 1 ps for further analysis. The results were visualized using pymol [56].

5. Acknowledgements

This work conducted by the Joint BioEnergy Institute was supported by the Office of Science, Office of Biological and Environmental Research, of the U.S. Department of Energy under Contract No. DE-AC02-05CH11231. This research used resources of the National Energy Research Scientific Computing Center (NERSC). We acknowledge Dr. Ping Yu at UC Davis for conducting solid state NMR measurements and Taylor Cu for the assistance in lab works.

467 ***Figure Captions***

468

469 **Fig. 1** Changes of cellulose crystallinity of **a)** switchgrass and **b)** Avicel solids pretreated by
470 [C_2mim][OAc]-water mixtures as revealed by PXRD.

471 **Fig 2**. **a)** Solid-state ^{13}C CP/MAS NMR and **b)** FTIR spectra of switchgrass pretreated by
472 [C_2mim][OAc]-water mixture

473 **Fig. 3** Enzymatic glucan digestibility of untreated switchgrass and switchgrass solids pretreated
474 by [C_2mim][OAc]-water mixtures at **a)** 5mg, and **b)** 20mg enzyme protein/g biomass.

475 **Fig. 4** Correlation between the initial enzymatic cellulose digestibility with **a)** lignin removal, **b)**
476 β value of the K-T parameters, **c)** CrI, **d)** xylan removal, and **e)** cellulose accessibility
477 derived from solid-state NMR.

478 **Fig. 5** Effect of [C_2mim][OAc]-water mixtures on disrupting the inter-chain H-bonds between
479 cellulose at 160 °C based on model simulation with cellulose I_β consisting 9 chains with
480 each chain having a polymerization of 6 glucose units.

481 **Fig. 6.** Analysis on dissecting the role of water interactions with (a) anion, (b) cellulose and (c)
482 cation in different [C_2mim][OAc]-water mixtures.

483

484

485

Table 1 Chemical composition, solid recovery, and component removal of switchgrass before and after pretreatment with [C_2mim][OAc]-water mixtures †

	Solid recovery, %	Glucan, %	Xylan, %	Klason lignin, %
Untreated	100.0	34.6±1.3	20.2±0.5	19.0±1.5
water-only	59.2±2.0	50.0±1.1 (6.0)	10.4±0.7 (69.6)	28.4±0.8 (11.5)
20% IL	59.8±1.1	48.5±2.6 (7.9)	13.9±2.3 (58.8)	21.3±1.0 (33.0)
50% IL	55.4±0.6	52.1±0.4 (8.3)	17.9±1.2 (50.9)	16.2±1.0 (52.7)
80% IL	51.4±1.3	55.0±1.4 (10.1)	14.5±0.9 (63.1)	15.7±2.4 (57.5)
100% IL	49.3±1.8	56.9±0.7 (11.0)	8.7±1.0 (78.8)	13.7±0.6 (64.6)

†Compositions reported for untreated sample are based on the dry weight of untreated biomass; Solid recoveries are based on the dry weight of untreated biomass, while the compositions for pretreated biomass are based on the dry weight of pretreated biomass; Values in parentheses are percentage removal of each component (glucan, xylan or lignin) during pretreatment based on its original amount in untreated biomass.

493 **Table 2** Solvent properties of [C_2mim][OAc]-water mixtures at 160 °C‡.

	pH		π: Solvent polarizability	α: Hydrogen bond donor capacity	β: Hydrogen bond acceptor capacity
	A	B			
water-only	6.86	4.09	0.67	1.46	0.97
20% IL	6.89	5.50	0.69	-	1.01
50% IL	8.15	6.22	0.73	0.88	1.04
80% IL	9.22	6.73	0.78	0.74	1.15
100% IL	11.55	7.13	0.84	0.51	1.23

494 ‡ π, α, and β parameters were extrapolated from actual measurement at 30, 60, 90, 110°C or up to 80°C
495 for water; the pH values were extrapolated from actual measurements of the 1:1 dilution of (A) the IL-
496 water mixtures and (B) the hydrolysate after pretreatment of switchgrass; (α) value of 20% [C_2mim][OAc]
497 in water could not be determined since no peak was observed with Reichardt's dye.

498

499

500 **Table 3** Elution time and relative molecular mass of lignin solublized during pretreatment using
501 [C_2mim][OAc]-water mixtures *

	Lignin solublized in pretreatment hydrolyzate			Lignin retained in untreated/pretreated solids		
Regions with elution time (min)	Excluded (%)	Retained (%)	$A_{E/R}$	Excluded (%)	Retained (%)	$A_{E/R}$
	t < 13.4 (u > 46k)	t < 13.4 (u > 46k)		t < 13.4 (u > 46k)	t < 13.4 (u > 46k)	
EMAL switchgrass	N/A	N/A	N/A	70.9	29.1	2.43
water-only	34.2	65.8	0.52	63.6	36.4	1.75
20% IL	41.3	58.7	0.70	66.5	33.5	1.99
50% IL	48.0	52.0	0.92	59.8	40.2	1.49
80% IL	41.0	59.0	0.69	58.5	41.5	1.41
100% IL	31.3	68.7	0.46	45.3	54.7	0.83

502 * $A_{E/R}$ stands for the ratio of peak areas in the excluded and retained regions; N/A stands for not available.

503

504

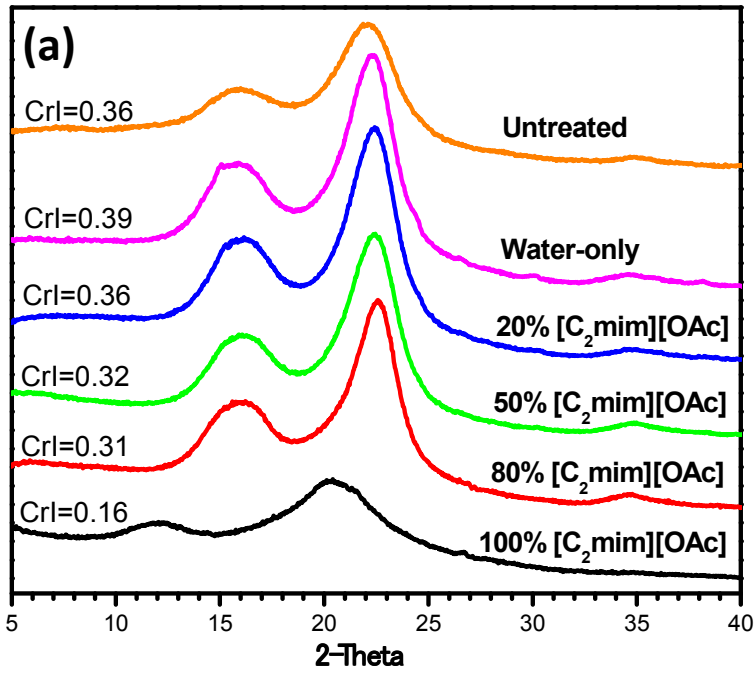

505

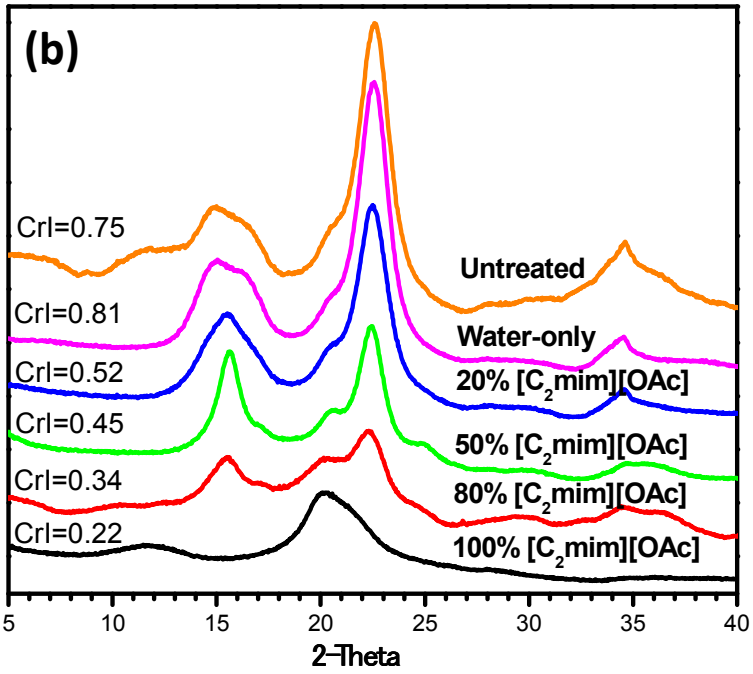

506

507 **Figure 1** Changes of cellulose crystallinity of **a)** switchgrass and **b)** Avicel solids pretreated by

508 [C_2mim][OAc]-water mixtures as revealed by pXRD.

509

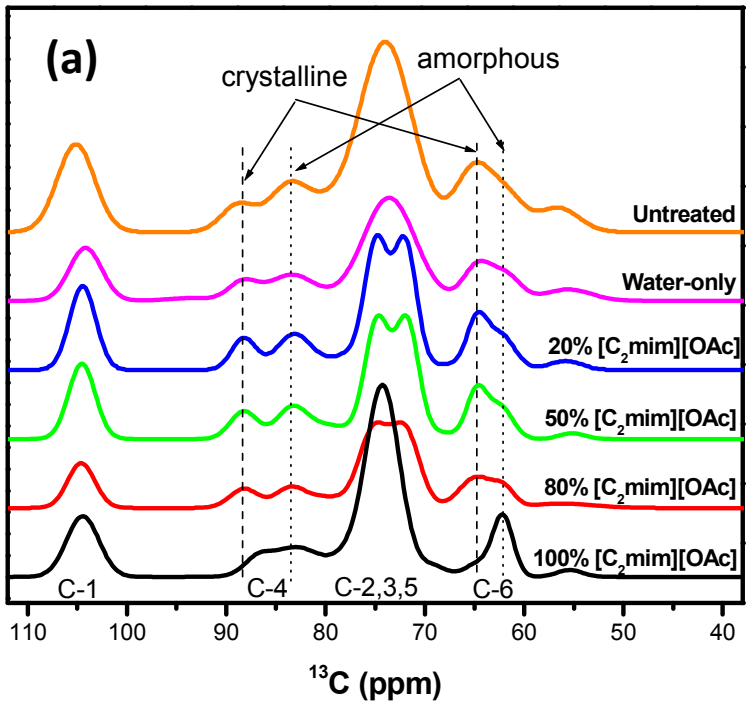

510

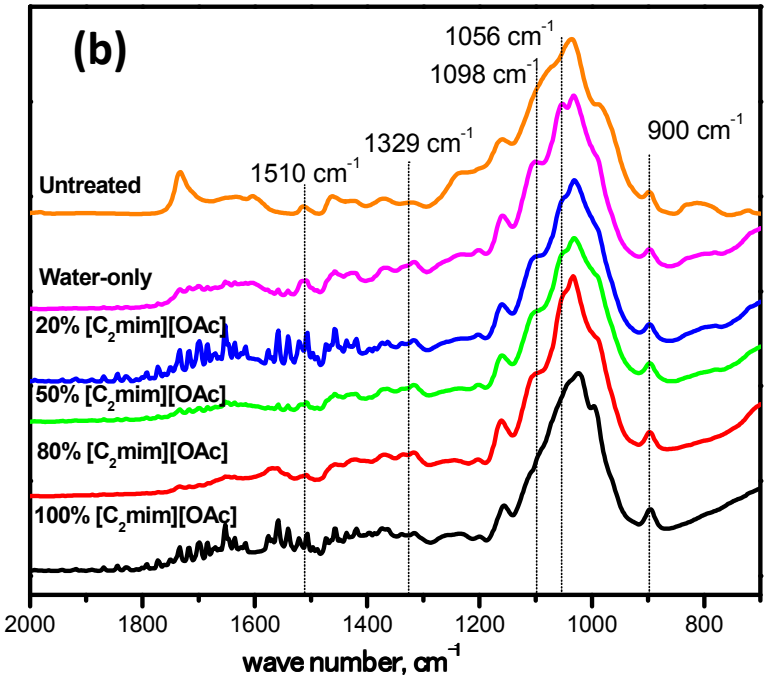

511

512 **Figure 2 a)** Solid-state ^{13}C CP/MAS NMR and **b)** FTIR spectra of switchgrass pretreated by

513 [C_2mim][OAc]-water mixture.

514

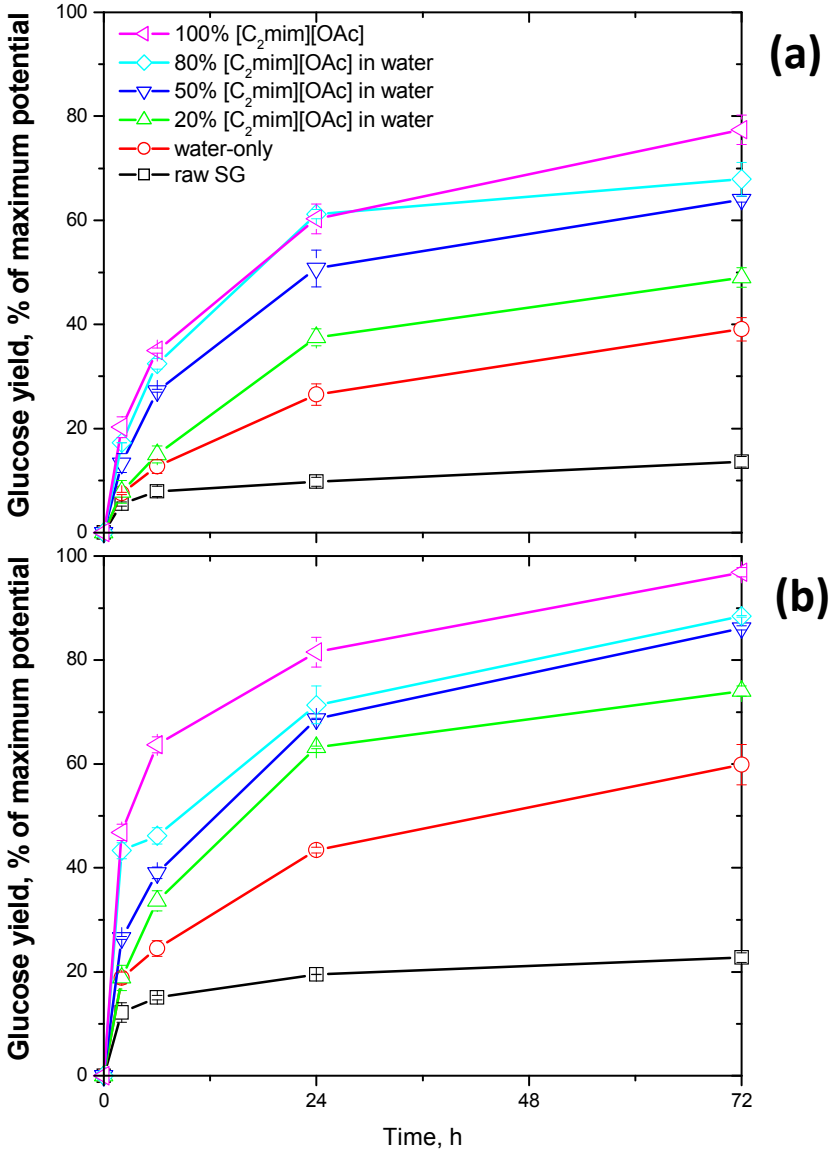

515

516

517 **Figure 3** Glucose yield from enzymatic hydrolysis of untreated switchgrass and switchgrass
518 solids pretreated by [C_2mim][OAc]-water mixtures at **a)** 5mg, and **b)** 20mg enzyme protein/g
519 initial biomass.

520

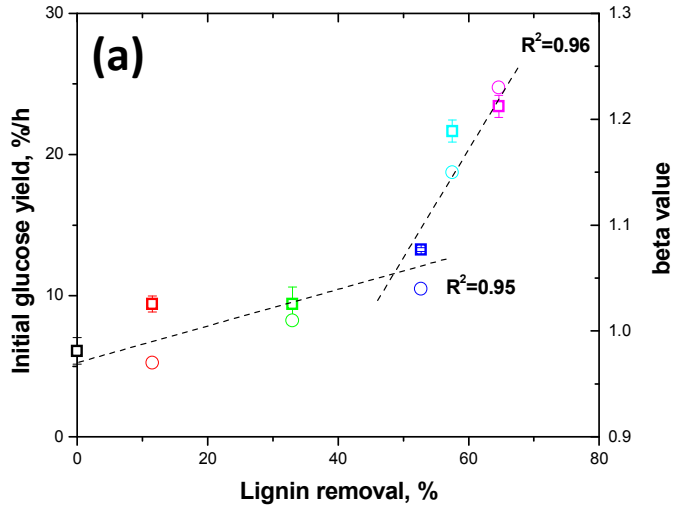

521

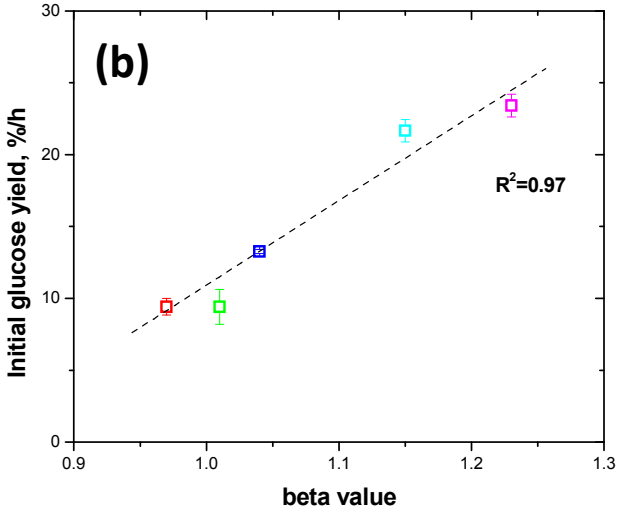

522

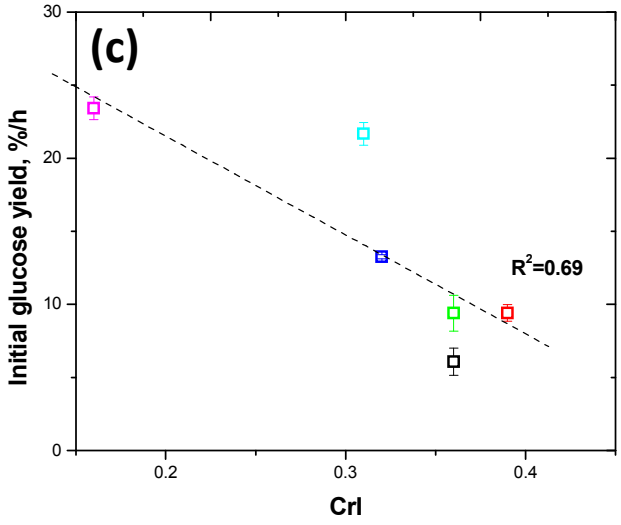

523

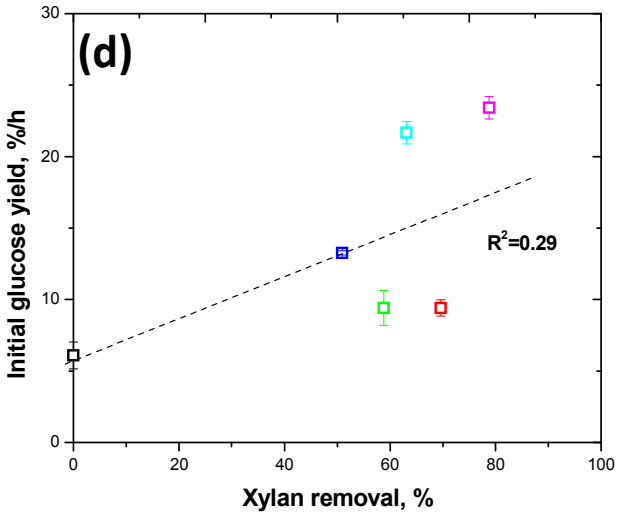

Figure 4 Correlation between the initial enzymatic cellulose digestibility with **a)** lignin removal, **b)** β value of the K-T parameters, **c)** CrI, **d)** xylan removal.

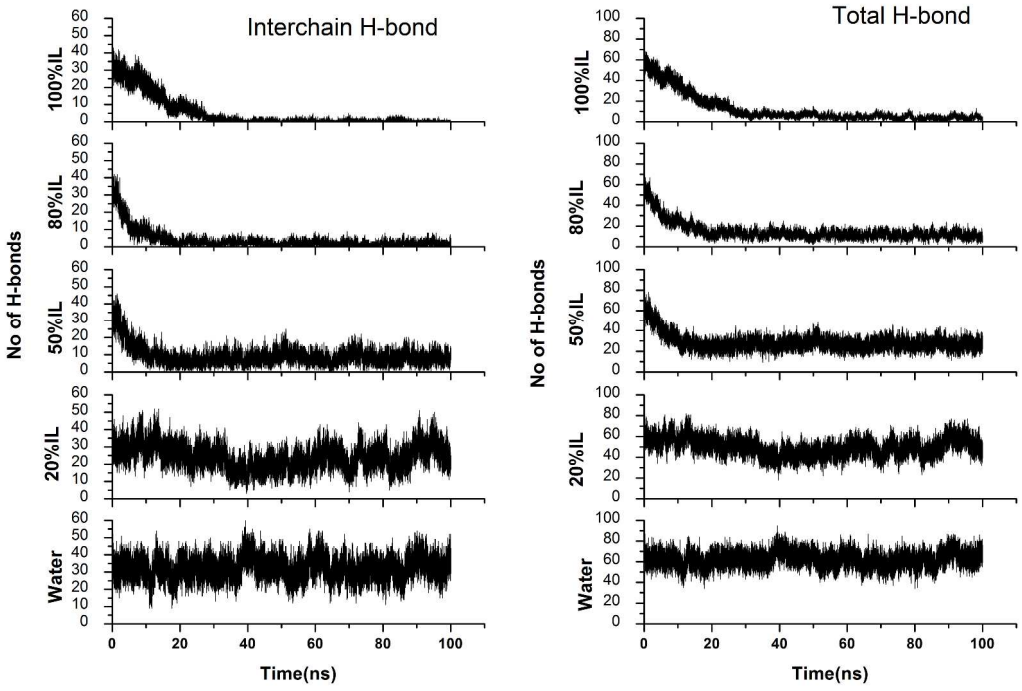

530

531 **Figure 5** Effect of [C_2mim][OAc]-water mixtures on disrupting the inter-chain H-bonds and

532 total H-bonds between cellulose at 160 °C based on model simulation with cellulose I_β

533 consisting 9 chains with each chain having a polymerization of 6 glucose units.

534

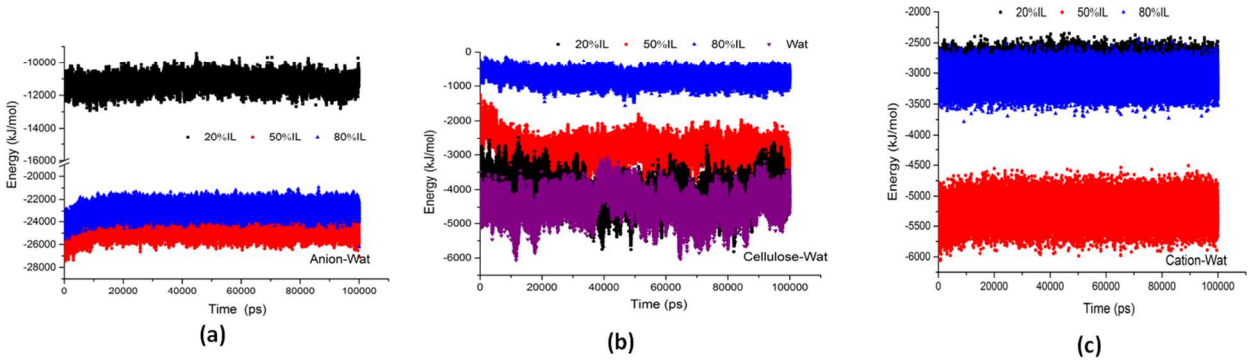

535
536 **Figure 6** Analysis on dissecting the role of water interactions with (a) anion, (b) cellulose and (c)
537 cation in different [C_2mim][OAc]-water mixtures.

538

6. References

1. M. E. Himmel, S. Y. Ding, D. K. Johnson, W. S. Adney, M. R. Nimlos, J. W. Brady and T. D. Foust, *Science*, 2007, **315**, 804-807.

2. J. Shi, M. A. Ebrik, B. Yang, R. J. Garlock, V. Balan, B. E. Dale, V. R. Pallapolu, Y. Y. Lee, Y. Kim, N. S. Mosier, M. R. Ladisch, M. T. Holtzapple, M. Falls, R. Sierra-Ramirez, B. S. Donohoe, T. B. Vinzant, R. T. Elander, B. Hames, S. Thomas, R. E. Warner and C. E. Wyman, *Bioresource Technology*, 2011, **102**, 11080-11088.

3. S. Singh, B. A. Simmons and K. P. Vogel, *Biotechnology and Bioengineering*, 2009, **104**, 68-75.

4. C. L. Li, B. Knierim, C. Manisseri, R. Arora, H. V. Scheller, M. Auer, K. P. Vogel, B. A. Simmons and S. Singh, *Bioresource Technology*, 2010, **101**, 4900-4906.

5. J. Shi, J. M. Gladden, N. Sathitsuksanoh, P. Kambam, L. Sandoval, D. Mitra, S. Zhang, A. George, S. W. Singer, B. A. Simmons and S. Singh, *Green Chemistry*, 2013, **15**, 2579-2589.

6. D. Klein-Marcuschamer, B. A. Simmons and H. W. Blanch, *Biofuels, Bioproducts & Biorefining*, 2011, **5**, 562-569.

7. S. Singh and B. A. Simmons, in *Aqueous Pretreatment of Plant Biomass for Biological and Chemical Conversion to Fuels and Chemicals*, ed. C. E. Wyman, 2013.

8. J. I. Park, E. J. Steen, H. Burd, S. S. Evans, A. M. Redding-Johnson, T. Batth, P. I. Benke, P. D'haeseleer, N. Sun, K. L. Sale, J. D. Keasling, T. S. Lee, C. J. Petzold, A. Mukhopadhyay, S. W. Singer, B. A. Simmons and J. M. Gladden, *Plos One*, 2012, **7**, e37010

9. J. M. Gladden, M. Allgaier, C. S. Miller, T. C. Hazen, J. S. VanderGheynst, P. Hugenholtz, B. A. Simmons and S. W. Singer, *Applied and Environmental Microbiology*, 2011, **77**, 5804-5812.

10. D. B. Fu and G. Mazza, *Bioresource Technology*, 2011, **102**, 8003-8010.

11. A. Brandt, M. J. Ray, T. Q. To, D. J. Leak, R. J. Murphy and T. Welton, *Green Chemistry*, 2011, **13**, 2489-2499.

12. X. D. Hou, N. Li and M. H. Zong, *Bioresource Technology*, 2013, **136**, 469-474.

13. H. Liu, K. L. Sale, B. M. Holmes, B. A. Simmons and S. Singh, *The Journal of Physical Chemistry B*, 2010, **114**, 4293-4301.

14. M. Abe, Y. Fukaya and H. Ohno, *Chemical Communications*, 2012, **48**, 1808-1810.

15. M. Mazza, D. A. Catana, C. Vaca-Garcia and C. Cecutti, *Cellulose*, 2009, **16**, 207-215.

16. K. M. Gupta, Z. Q. Hu and J. W. Jiang, *Rsc Advances*, 2013, **3**, 4425-4433.

17. F. Huo, Z. P. Liu and W. C. Wang, *Journal of Physical Chemistry B*, 2013, **117**, 11780-11792.

18. T. V. Doherty, M. Mora-Pale, S. E. Foley, R. J. Linhardt and J. S. Dordick, *Green Chemistry*, 2010, **12**, 1967-1975.

19. N. Sun, R. Parthasarathi, A. M. Socha, J. Shi, S. Zhang, V. Stavila, K. L. Sale, B. A. Simmons and S. Singh, *Green Chemistry*, 2014, **16**, 2546-2557.

20. P. Kilpelainen, V. Kitunen, A. Pranovich, H. Ilvesniemi and S. Willfor, *Bioresources*, 2013, **8**, 5202-5218.

21. G. Papa, P. Varanasi, L. Sun, G. Cheng, V. Stavila, B. Holmes, B. A. Simmons, F. Adani and S. Singh, *Bioresource Technology*, 2012, **117**, 352-359.

22. P. Varanasi, P. Singh, R. Arora, P. D. Adams, M. Auer, B. A. Simmons and S. Singh, *Bioresour Technol*, 2012, **126**, 156-161.

23. P. Mansikkamäki, M. Lahtinen and K. Rissanen, *Cellulose*, 2005, **12**, 233-242.

24. G. Cheng, P. Varanasi, C. L. Li, H. B. Liu, Y. B. Menichenko, B. A. Simmons, M. S. Kent and S. Singh, *Biomacromolecules*, 2011, **12**, 933-941.

25. M. J. Kamlet and R. Taft, *Journal of the American Chemical Society*, 1976, **98**, 377-383.

26. C. Reichardt, *Pure and applied chemistry*, 2004, **76**, 1903-1919.

27. T. V. Doherty, M. Mora-Pale, S. E. Foley, R. J. Linhardt and J. S. Dordick, *Green Chem.*, 2010, **12**, 1967-1975.

28. M. Ab Rani, A. Brant, L. Crowhurst, A. Dolan, M. Lui, N. Hassan, J. Hallett, P. Hunt, H. Niedermeyer and J. Perez-Arlandis, *Physical Chemistry Chemical Physics*, 2011, **13**, 16831-16840.

29. Y. Fukaya, K. Hayashi, M. Wada and H. Ohno, *Green Chemistry*, 2008, **10**, 44-46.

30. H. Ohno and Y. Fukaya, *Chemistry Letters*, 2009, **38**, 2-7.

31. A. Xu, J. Wang and H. Wang, *Green Chemistry*, 2010, **12**, 268-275.

32. L. K. J. Hauru, M. Hummel, A. W. T. King, I. A. Kilpeläinen and H. Sixta, *Biomacromolecules*, 2012, **13**, 2896–2905.

33. J. Kahlen and K. Leonhard, *Green Chemistry*, 2010, **12**, 2172-2181.

34. M. G. S. Chua and M. Wayman, *Canadian Journal of Chemistry-Revue Canadienne De Chimie*, 1979, **57**, 1141-1149.

35. J. B. Li, G. Henriksson and G. Gellerstedt, *Bioresource Technology*, 2007, **98**, 3061-3068.

36. H. L. Trajano, N. L. Engle, M. Foston, A. J. Ragauskas, T. J. Tschaplinski and C. E. Wyman, *Biotechnology for Biofuels*, 2013, **6**.

37. N. Sathitsuksanoh, K. M. Holtman, D. J. Yelle, T. Morgan, V. Stavila, J. Pelton, H. Blanch, B. A. Simmons and A. George, *Green Chemistry*, 2014, **16**, 1236-1247.

38. J. L. Wen, T. Q. Yuan, S. L. Sun, F. Xu and R. C. Sun, *Green Chemistry*, 2014, **16**, 181-190.

39. A. George, K. Tran, T. J. Morgan, P. I. Benke, C. Berrueco, E. Lorente, B. C. Wu, J. D. Keasling, B. A. Simmons and B. M. Holmes, *Green Chemistry*, 2011, **13**, 3375-3385.

40. R. H. Newman and J. A. Hemmingson, *Cellulose*, 1995, **2**, 95-110.

41. S. Park, D. K. Johnson, C. I. Ishizawa, P. A. Parilla and M. F. Davis, *Cellulose*, 2009, **16**, 641-647.

42. S. Park, J. O. Baker, M. E. Himmel, P. A. Parilla and D. K. Johnson, *Biotechnology for Biofuels*, 2010, **3**.

43. N. Sathitsuksanoh, Z. G. Zhu, S. Wi and Y. H. P. Zhang, *Biotechnology and Bioengineering*, 2011, **108**, 521-529.

44. R. Arora, C. Manisseri, C. L. Li, M. D. Ong, H. V. Scheller, K. Vogel, B. A. Simmons and S. Singh, *Bioenergy Research*, 2010, **3**, 134-145.

45. D. B. Fu and G. Mazza, *Bioresource Technology*, 2011, **102**, 7008-7011.

46. R. Kumar, G. Mago, V. Balan and C. E. Wyman, *Bioresource Technology*, 2009, **100**, 3948-3962.

47. R. C. Remsing, R. P. Swatloski, R. D. Rogers and G. Moyna, *Chem. Commun.*, 2006, 1271-1273.

48. J. B. Taylor, *Transactions of the Faraday Society*, 1957, **53**, 1198-1203.

49. A. E. Bennett, C. M. Rienstra, M. Auger, K. V. Lakshmi and R. G. Griffin, *Journal of Chemical Physics*, 1995, **103**, 6951-6958.

50. M. Selig, N. Weiss and Y. Ji, Technical Report, NREL/TP-510-42629. National Renewable Energy Laboratory, Golden, CO, 2008.

51. A. Sluiter, B. Hames, R. Ruiz, J. Sluiter, D. Templeton and D. Crocker, Technical Report, NREL/TP-510-42618. National Renewable Energy Laboratory, Golden, CO, 2008.

52. A. Guerra, I. Filpponen, L. A. Lucia and D. S. Argyropoulos, *Journal of Agricultural and Food Chemistry*, 2006, **54**, 9696-9705.

632 53. H. J. C. Berendsen, D. Vanderspoel and R. Vandrunen, *Computer Physics Communications*,
633 1995, **91**, 43-56.

634 54. B. Hess, C. Kutzner, D. van der Spoel and E. Lindahl, *Journal of Chemical Theory and*
635 *Computation*, 2008, **4**, 435-447.

636 55. R. J. Woods, R. A. Dwek, C. J. Edge and B. Fraserreid, *Journal of Physical Chemistry*, 1995,
637 **99**, 3832-3846.

638 56. J. M. Wang, R. M. Wolf, J. W. Caldwell, P. A. Kollman and D. A. Case, *Journal of*
639 *Computational Chemistry*, 2004, **25**, 1157-1174.

640 57. W. L. Jorgensen, J. Chandrasekhar, J. D. Madura, R. W. Impey and M. L. Klein, *Journal of*
641 *Chemical Physics*, 1983, **79**, 926-935.

642 58. T. Darden, D. York and L. Pedersen, *Journal of Chemical Physics*, 1993, **98**, 10089-10092.

643 59. B. Hess, H. Bekker, H. J. C. Berendsen and J. G. E. M. Fraaije, *Journal of Computational*
644 *Chemistry*, 1997, **18**, 1463-1472.

645 60. S. Nose and M. L. Klein, *Molecular Physics*, 1983, **50**, 1055-1076.

646

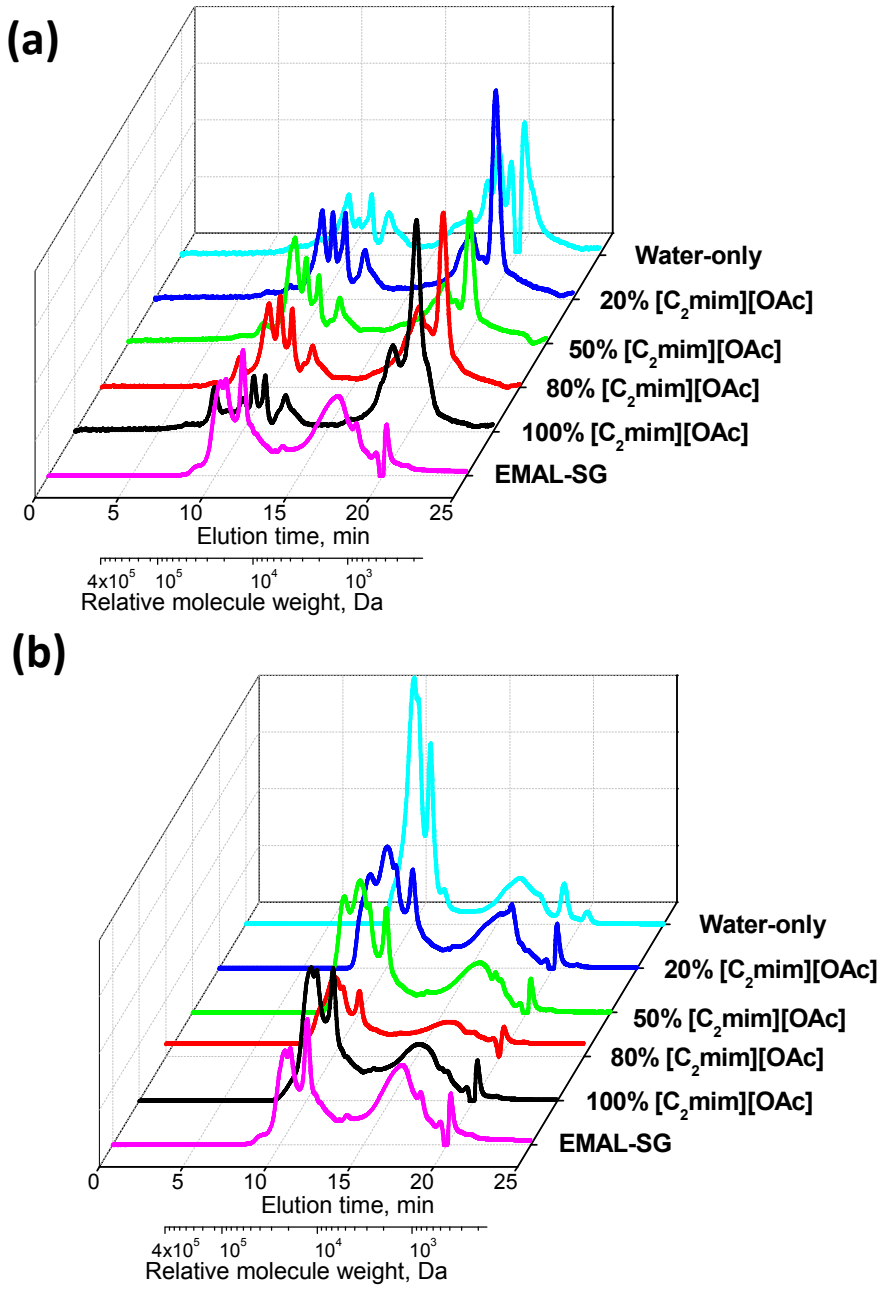

Figure S1 Area-normalized size exclusion chromatography (SEC) of lignin **a)** solublized in aqueous [C_2mim][OAc] and **b)** retained in pretreated solids by [C_2mim][OAc]-water mixtures at 160 °C for 3h using EMAL of untreated switchgrass as a control. See **Table 3** for relative area of excluded and retained regions.

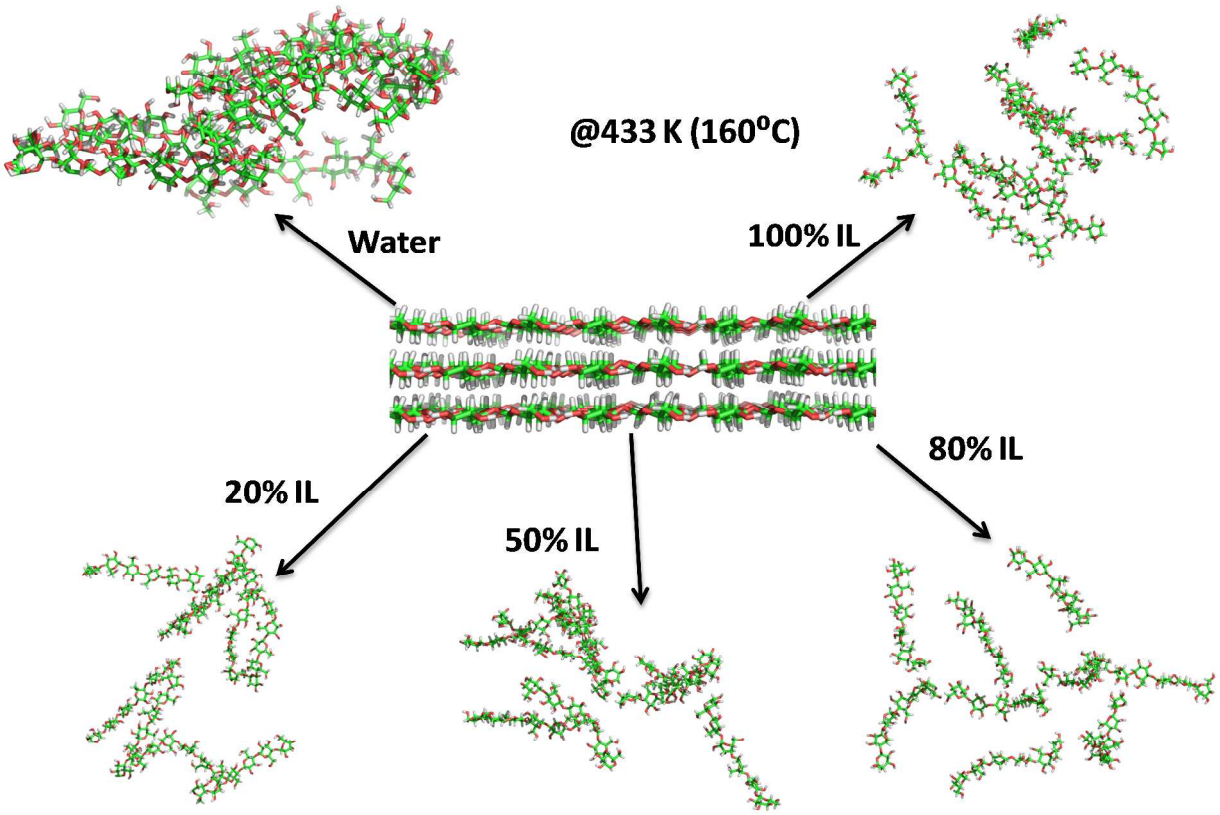

Figure S2 Diagram of the model simulation results showing the effect of [C_2mim][OAc]-water mixtures on disrupting a representative cellulose I_β substructure consisting 9 chains with each chain having a polymerization of 6 glucose units at 160 °C.

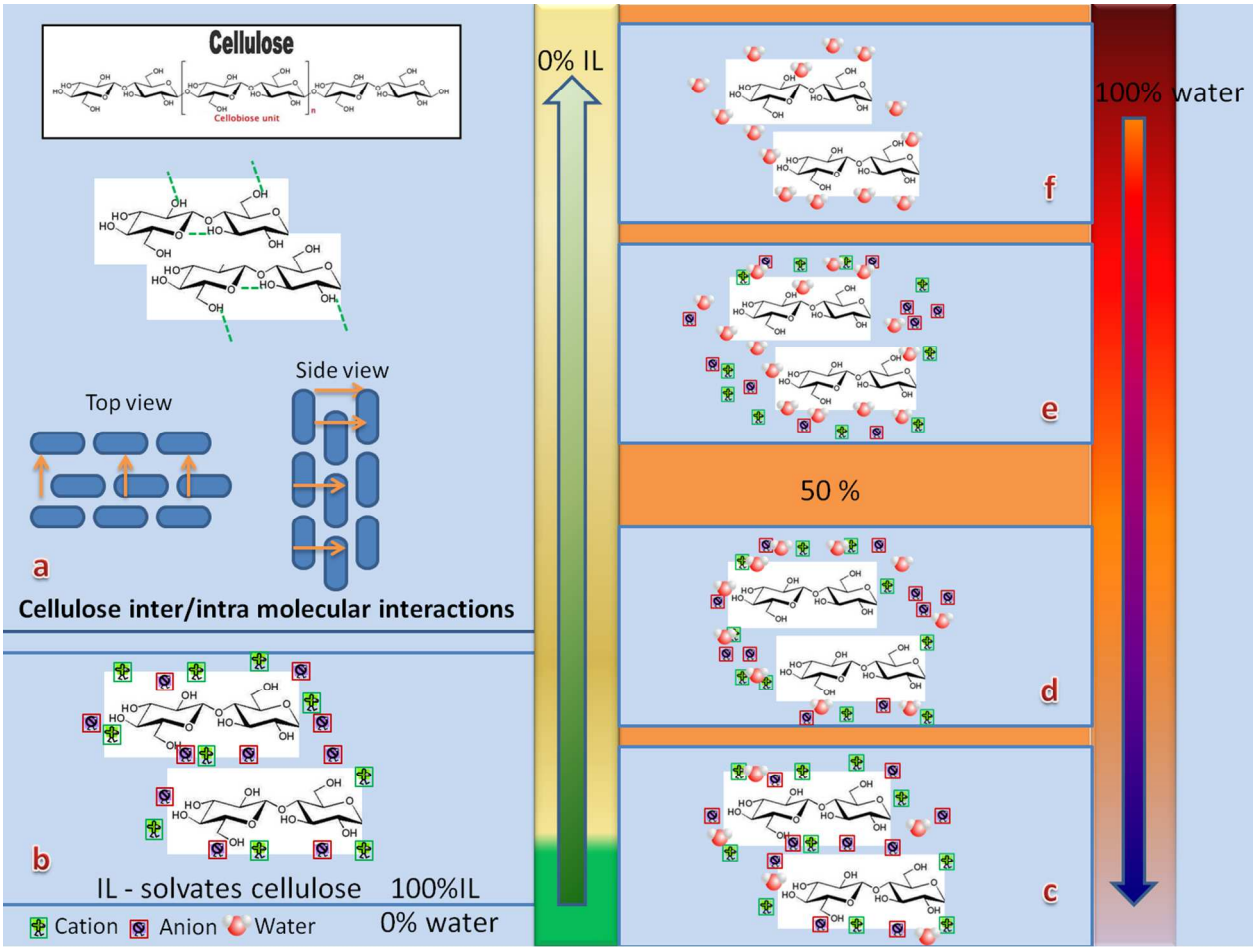

Figure S3 Schematics of [C_2mim][OAc]-water dissolution process – **(a)** cellulose structure showing inter/intramolecular interactions; **(b)** IL solvates cellulose; **(c & d)** water in [C_2mim][OAc] and assisting the dissolution process (below 50 % ratio of water in [C_2mim][OAc] act as co-solvent) **(e)** above 50 % ratio of water in [C_2mim][OAc] solvates ions and reduces cellulose dissolution; **(f)** water solvates cellulose.

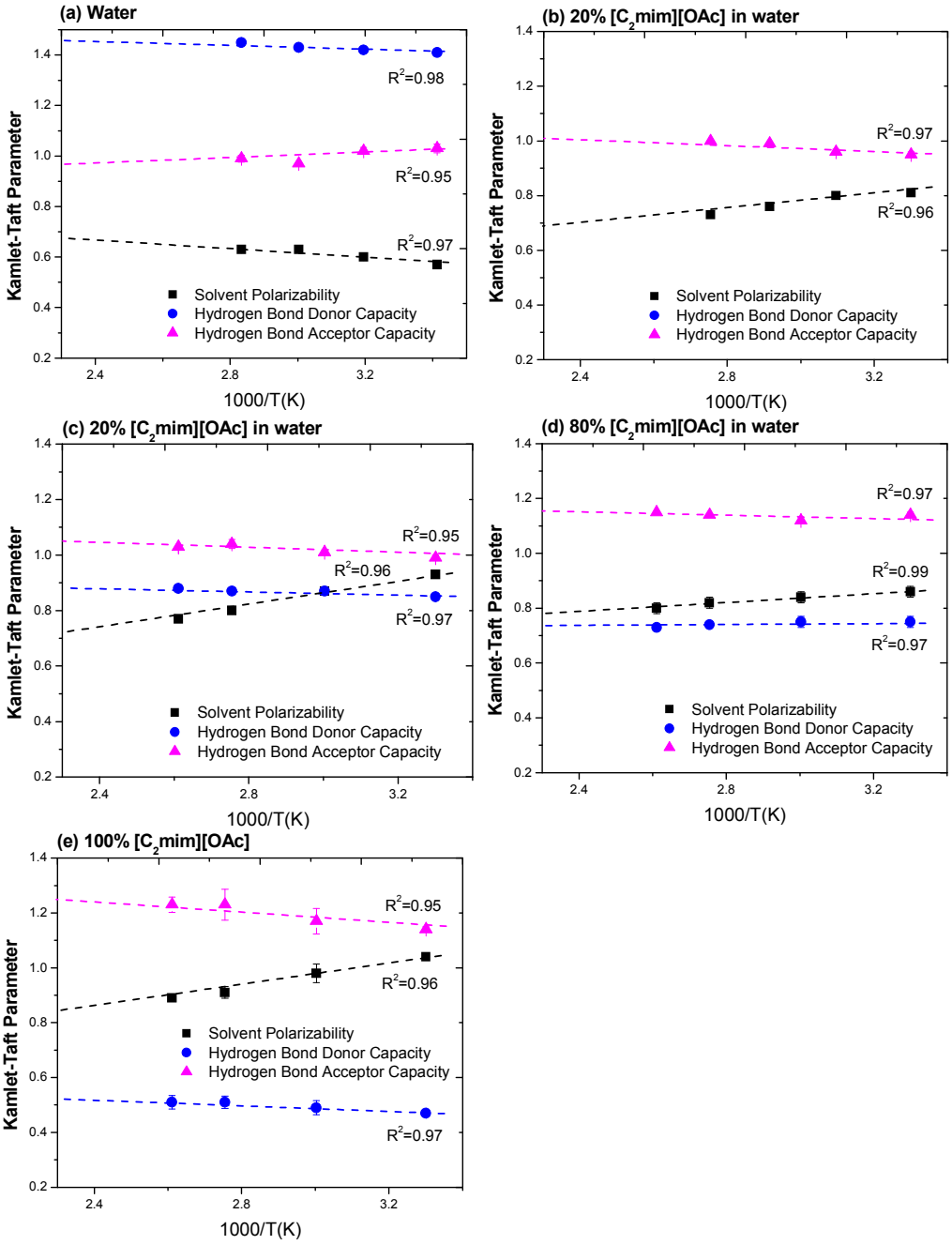

668

669

670

671 **Figure S4** Extrapolation of Kamlet-Taft values of [C_2mim][OAc]-water mixture (the Y-intercept

672 indicates the extrapolated K-T parameters at 1000/T(K)=2.31 or 160 °C).

673

Table of Contents

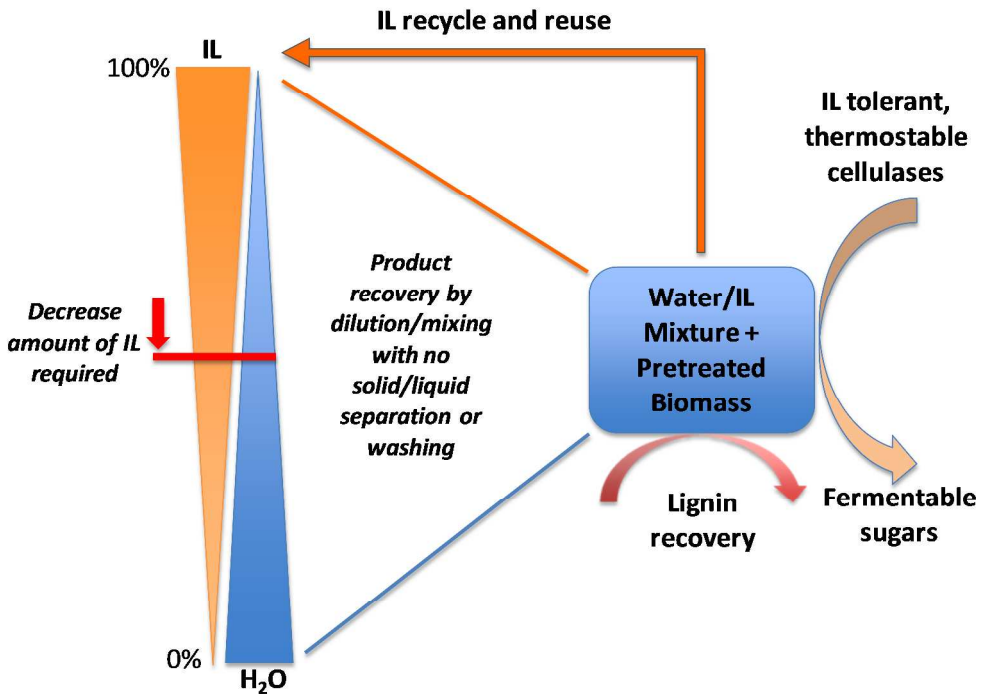

Pretreatment with aqueous IL.